
Wide-Field Choroidal Thickness Analysis after Half-fluence Photodynamic Therapy in Pachychoroid Neovascularopathy

Yosuke Fukuda , [Shoji Notomi](#) * , Satomi Shiose , Yusuke Maehara , Kohei Kiyohara , Sawako Hashimoto ,
Kumiko Kano , Keijiro Ishikawa , [Toshio Hisatomi](#) , Koh-Hei Sonoda

Posted Date: 29 January 2024

doi: 10.20944/preprints202401.2015.v1

Keywords: age-related macular degeneration; pachychoroid neovascularopathy; photodynamic therapy; anti-vascular endothelial growth factor therapy; ultra-wide-field optical coherent tomography



Preprints.org is a free multidiscipline platform providing preprint service that is dedicated to making early versions of research outputs permanently available and citable. Preprints posted at Preprints.org appear in Web of Science, Crossref, Google Scholar, Scilit, Europe PMC.

Copyright: This is an open access article distributed under the Creative Commons Attribution License which permits unrestricted use, distribution, and reproduction in any medium, provided the original work is properly cited.

Article

Wide-Field Choroidal Thickness Analysis after Half-fluence Photodynamic Therapy in Pachychoroid Neovascularopathy

Yosuke Fukuda ¹, Shoji Notomi ^{1*}, Satomi Shiose ¹, Yusuke Maehara ¹, Kohei Kiyohara ¹, Sawako Hashimoto ¹, Kumiko Kano ¹, Keijiro Ishikawa ¹, Toshio Hisatomi ² and Koh-Hei Sonoda ¹.

¹ Department of Ophthalmology, Graduate School of Medical Sciences, Kyushu University, 3-1-1 Maidashi, Higashi-Ku, Fukuoka 812-8582, Japan

² Department of Ophthalmology, Fukuoka University Chikushi Hospital, 1-1-1 Zokumyoin, Chikushino, Fukuoka 818-8502, Japan

* Correspondence: Shoji Notomi, e-mail: noutomi.shouji.926@m.kyushu-u.ac.jp

Abstract: Pachychoroid neovascularopathy (PNV) is a pachychoroid-spectrum disease. As blood circulation throughout the choroid may be involved in PNV pathogenesis, analysis using ultra-wide-field (UWF) fundus imaging is crucial. We evaluated choroidal thickness after half-fluence photodynamic therapy (PDT) combined with intravitreal aflibercept injection for PNV using UWF swept-source optical coherence tomography. Seventeen eyes with PNV that underwent half-fluence PDT with adjuvant single intravitreal aflibercept injection were analyzed. To compare choroidal thicknesses in the central and peripheral choroids, we set subfields <3, <9, and 9–18 mm from the fovea. The <9- and 9–18-mm subfields were divided into four quadrants. Choroidal thickness in each subfield decreased significantly after half-fluence PDT ($P < 0.001$); this reduction was more pronounced in the central area. We also investigated the relationship between the dominant side of the deep choroidal veins that harbor choroidal vein efflux from the macula. When choroidal thickness in the supratemporal and infratemporal 9x9-mm subfields were evaluated, the ratio of choroidal thickness reduction was not significantly different between the dominant and non-dominant sides. The dominant side was not associated with the extent of choroidal thickness reduction in PNV. In conclusion, half-fluence PDT caused thinning of the entire choroid, especially in the central area, in PNV.

Keywords: age-related macular degeneration; pachychoroid neovascularopathy; photodynamic therapy; anti-vascular endothelial growth factor therapy; ultra-wide-field optical coherent tomography

1. Introduction

Pachychoroid neovascularopathy (PNV), a type of pachychoroid-spectrum disease (PSD), is a subtype of neovascular age-related macular degeneration (nAMD). PNV is associated with characteristics of PSD, such as choroidal thickening, dilated choroidal vessels, and choroidal vascular hyperpermeability (CVH) [1-4]. Similar to central serous chorioretinopathy (CSC), PNV is accompanied by a thickened choroid, especially in the posterior pole, unlike other subtypes of nAMD [5-7]. While CSC is associated with pachychoroid-driven leakage through the breakdown of the retinal pigment epithelium (RPE) barrier, similar choroidal pathology may also lead to the development of macular neovascularization (MNV) [8].

Although anti-VEGF therapy is effective against PNV, several studies have shown that patients require frequent clinical visits and repeated intravitreal injections [9-11]. Photodynamic therapy (PDT) has been demonstrated to resolve the subretinal fluid (SRF) in CSC [12, 13], suggesting that PDT could be effective against PNV. Indeed, the combination of half dose/fluence PDT with anti-VEGF therapy has been shown to reduce the need for frequent injection regimens for PNV [14, 15].

Dysregulation of choroidal circulation, which normally drains through the vortex vein ampulla, has been suggested to play a role in the pathology of PSD [16]. Therefore, assessing choroidal

thickness, including that of the peripheral choroid, is important in PSD studies. A study showed that eyes affected by CSC demonstrated a higher frequency of vertical asymmetry in the running pattern of the deep choroidal veins compared to that in those of healthy participants [17]. Although this asymmetry is observed in healthy individuals, it is believed to play a role in the pathology of PSD.

Ultrawide-field optical coherence tomography (UWF-OCT) facilitates the measurement of choroidal thickness in the peripheral regions. Our previous study demonstrated that the choroidal thickness in PNV exceeds that in other nAMD subtypes, even after adjusting for axial length and age [5]. Although recent studies have documented changes in choroidal thickness following PDT in CSC using UWF-OCT [18-20], such evidence remains limited for PNV. This study aimed to analyze variations in choroidal thickness after half-fluence PDT for PNV using UWF-OCT.

2. Materials and Methods

2.1. Patients

This retrospective study was approved by the Institutional Review Board of Kyushu University, Fukuoka, Japan (approval number: 2019-630), and adhered to the tenets of the Declaration of Helsinki. All data were anonymized prior to analysis. We included patients with treatment-naïve PNV who visited Kyushu University Hospital between March 2021 and June 2023 and underwent half-fluence PDT with 6 mg/m² verteporfin. The diagnosis of PNV was based on the absence of large drusen and the presence of either CVH or dilated choroidal vessels. In addition, PNV diagnosis was defined by the presence of type 1 MNV, as visualized using OCT angiography. Patients with polypoidal lesions and those with a history of treatment for PNV were excluded. All patients received an adjuvant single intravitreal injection of 2.0 mg/0.05 mL aflibercept (EYLEA®; Regeneron Pharmaceutical Inc and Bayer, Tarrytown, NY, USA) prior to PDT. Half-fluence PDT was performed 1 week after administering the intravitreal injection of aflibercept. Fifteen minutes after initiating intravenous verteporfin infusion, a 689-nm laser was applied for 83 seconds to deliver 25 J/cm². The greatest linear dimension (GLD) was determined to cover the abnormal vascular network.

At the initial presentation, all patients underwent comprehensive ophthalmic examination of both eyes including best-corrected visual acuity (BCVA) using the Landolt chart, slit-lamp biomicroscopy, intraocular pressure, color fundus photography covering the 45-degree posterior retina, fluorescein/indocyanine-green angiography, near-infrared reflectance, fundus autofluorescence (HRA-II; Heidelberg Engineering, Dossenheim, Germany), spectral-domain OCT (Spectralis HRA + OCT or Cirrus™ 5000 HD-OCT; Zeiss, Dublin, CA), and UWF swept-source OCT (Xephilio OCT-S1; Canon Medical Systems, Tokyo, Japan). OCT angiography was performed using the AngioVue Imaging System (Optovue Inc., Fremont, CA, USA). All patients underwent a follow-up examination using UWF swept-source OCT 3 months after half-fluence PDT.

2.2. Evaluation of choroidal thickness via UWF swept-source OCT

Central and peripheral choroidal thicknesses were analyzed as previously described [5, 6]. Briefly, we acquired three-dimensional volume data with vertical dimensions of 20 mm, horizontal dimensions of 23 mm, and scan depth 5.3 mm using UWF swept-source OCT. For segmentation of the choroid, we set the choroidal thickness as the vertical distance from the Bruch's membrane to the choriocleral interface. Segmentation was automatically performed using the built-in software (Xephilio OCT-S1) and manual correction when required. For a more accurate evaluation of the wide-field choroidal thicknesses, we performed an automatic real-shape correction on the acquired OCT images using the software provided by Canon Inc. (US patent 9149181 B2).

To compare the central and peripheral choroidal thicknesses, we set a grid consisting of three circles with diameters of 3, 9, and 18 mm, centered on the fovea. Three subfields were set up in this study as follows: (a) <3 mm, (b) <9 mm, and (c) 9–18 mm (**Figure 1A and B**). Furthermore, to examine changes in choroidal thickness before and after treatment in detail, we divided 3-9 mm-subfield and 9-18 mm-subfield into four quadrants: supratemporal, infratemporal, supranasal, and infranasal (**Figure 1C**).

Three authors (S. N., S. S., and Y. F.) evaluated the presence of asymmetry and the dominant and non-dominant sides of the vortex veins for each patient with PSD. The dominant or non-dominant side of the vortex vein was determined by the deviation of the temporal horizontal watershed zone on en face UWF OCT images and was categorized into the asymmetrical (upper or lower dominant) and symmetrical groups (**Figure 2**). To assess choroidal thickness, including areas near the vortex vein ampulla, we set a 9x9-mm area located supra/inferotemporally from the fovea, with the fovea as one of its corners (**Figure 1D**). Changes in choroidal thickness were compared between the dominant and non-dominant sides.

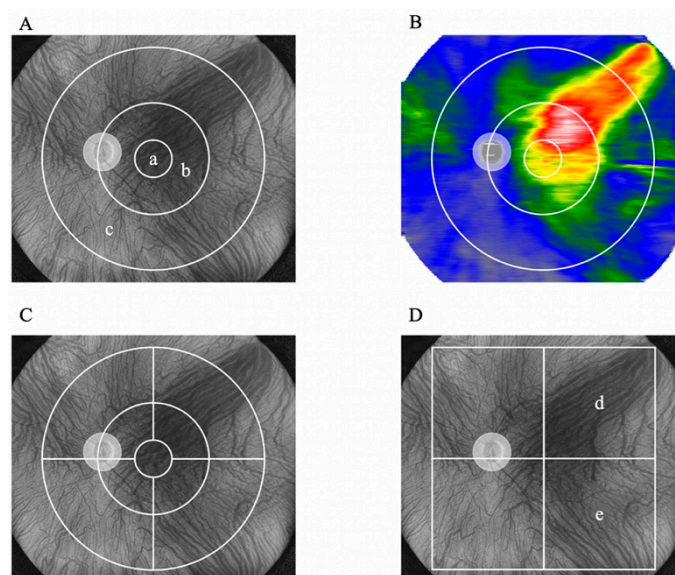


Figure 1. Choroidal thickness map and subfields. Representative images of the subfields and choroidal thickness maps obtained using UWF-OCT. (A) Three subfields, 3 mm (a), 9 mm (b), and 9–18 mm (c), are illustrated on an en face UWF-OCT image. (B) Representative image of the choroidal thickness map calculated from the Bruch’s membrane to chorioscleral interface in UWF OCT b-scans. (C) The 3–9- and 9–18-mm subfields were divided into four subfields. (D) Four square subfields were set, and the supratemporal (d) and infratemporal (e) 9x9-mm subfields were analyzed. UWF-OCT: ultrawide-field optical coherence tomography.

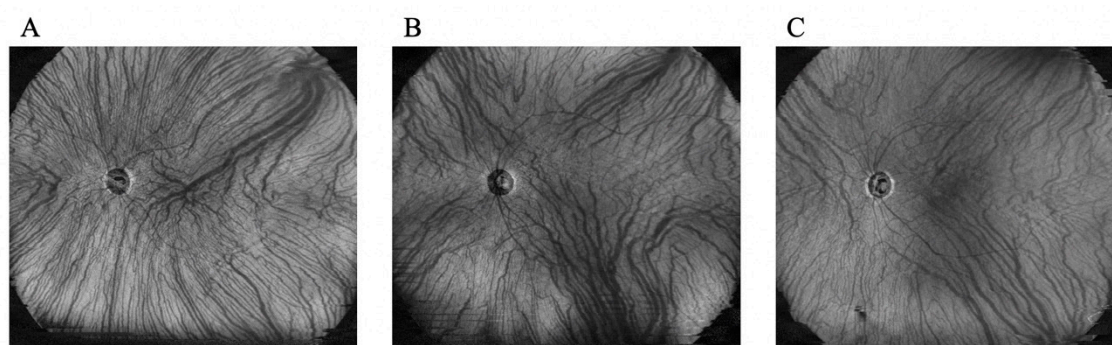


Figure 2. Symmetrical and asymmetrical patterns of deep choroidal veins and the vortex vein in en face images. Representative cases from each of the three groups: upper dominant (A), lower dominant (B), and asymmetrical (C).

2.3. Statistical analyses

Choroidal thickness in each subfield was measured before and 3 months after PDT. The patients were divided into two groups according to the presence of persistent SRF. We used the Mann-Whitney U test or Fisher's exact test for analyzing differences in patient background or choroidal thickness between the groups. The Wilcoxon signed-rank test was performed to compare changes in choroidal thickness and BCVA after treatment. Statistical significance was set at a P-value of 0.05.

3. Results

3.1. Characteristics of the enrolled patients

Seventeen eyes from 16 patients (including nine men and seven women) were analyzed in the study. The mean \pm standard deviation (SD) age was 65.1 ± 12.5 years. The mean \pm SD axial length was 24.3 ± 1.1 mm, and the mean \pm SD GLD was 3500 ± 905 μm . The mean \pm SD baseline BCVA was 0.15 ± 0.20 logarithm of the minimum angle of resolution (logMAR), and the mean \pm SD central retinal thickness was 335.1 ± 73.7 μm . There were eight eyes (47.1%) in the upper dominant group, three in the lower dominant group, and six in the asymmetrical group (Table 1). SRF was present before treatment in all cases.

Table 1. Patients' characteristics before treatment.

	17 eyes of 16 patients, n (%) or mean \pm SD
Male	9 (56.3 %)
Age (y)	65.1 ± 12.5
Axial length (mm)	24.3 ± 1.1
BCVA (logMAR)	0.15 ± 0.20
GLD (μm)	3500 ± 905
CMT (μm)	335.1 ± 73.7
Dominant side of deep choroidal veins	
Upper dominant	8 (47.1%)
Lower dominant	3 (17.6%)
Asymmetry	6 (35.3%)

SD: standard deviation, BCVA: best-corrected visual acuity, logMAR: logarithm of the minimum angle of resolution, GLD: greatest linear dimension, CMT: central macular thickness.

3.2. Treatment outcome and factors related to the presence of SRF after treatment

Of 17 eyes, residual or recurrent SRF was observed in seven eyes 3 months after treatment. In one eye, SRF was observed within the first 3 months after treatment. However, in all cases, including this one, no additional PDT or an additional injection of an anti-VEGF drug was administered within the initial 3 months post-treatment. Additionally, in one eye, SRF was observed 1 month after treatment but disappeared without additional treatment 2 months after treatment.

We examined factors related to the presence or absence of SRF 3 months after treatment; however, no significant differences in patient background were observed (Table 2). Despite the absence of significant differences, the group in which SRF was observed 3 months after treatment tended to be older before treatment ($P=0.11$). Furthermore, there was no significant difference in BCVA before and after treatment, and this did not vary according to the presence or absence of SRF 3 months after treatment (Figure 3). Overall, CMT decreased significantly after treatment, and this decrease was not dependent on the presence or absence of SRF 3 months after treatment (Figure 4).

Table 2. Factors related to the presence of SRF after treatment.

	SRF (-)	SRF (+)	P-value
n	10	7	
Male	6 (60.0%)	4 (56.3%)	0.64
Age (y)	61.0 ± 11.1	71.0 ± 12.5	0.11
Axial length (mm)	24.4 ± 0.8	24.2 ± 1.4	0.64
BCVA (logMAR)	0.17 ± 0.22	0.14 ± 0.18	0.76
GLD (μm)	3620 ± 980	3329 ± 828	0.53
CMT (μm)	326.7 ± 64.6	347.1 ± 89.2	0.59
Asymmetry of vortex vein			0.83
Upper dominant	4 (40.0%)	4 (57.1%)	
Lower dominant	2 (20.0%)	1 (14.3%)	
Asymmetry	4 (40.0%)	2 (28.6%)	

P-values were calculated using Fisher's exact test for ordinal data and the Mann-Whitney U test for continuous data. SRF: subretinal fluid, BCVA: best-corrected visual acuity, logMAR: logarithm of the minimum angle of resolution, GLD: greatest linear dimension, CMT: central macular thickness.

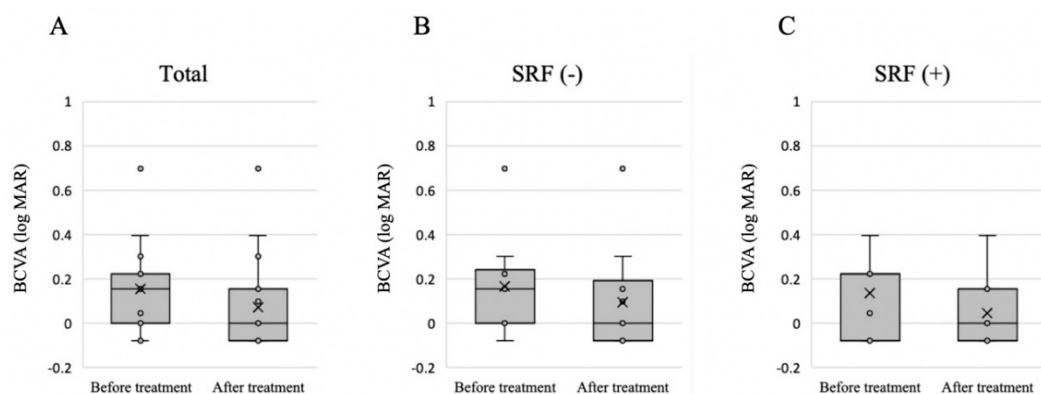


Figure 3. Changes in BCVA before and 3 months after treatment. (A) Changes in BCVA in all 17 eyes. The mean BCVA significantly improved after the treatment ($P = 0.02$, Wilcoxon signed rank test). (B) Changes in BCVA in 10 eyes with no SRF at 3 months after treatment. No significant difference in BCVA was observed before and after treatment ($P = 0.07$). (C) Changes in BCVA in seven eyes with SRF at 3 months after treatment. No significant difference in BCVA was observed before and after treatment ($P = 0.09$). BCVA: best-corrected visual acuity, SRF: subretinal fluid, logMAR: logarithm of the minimum angle of resolution.

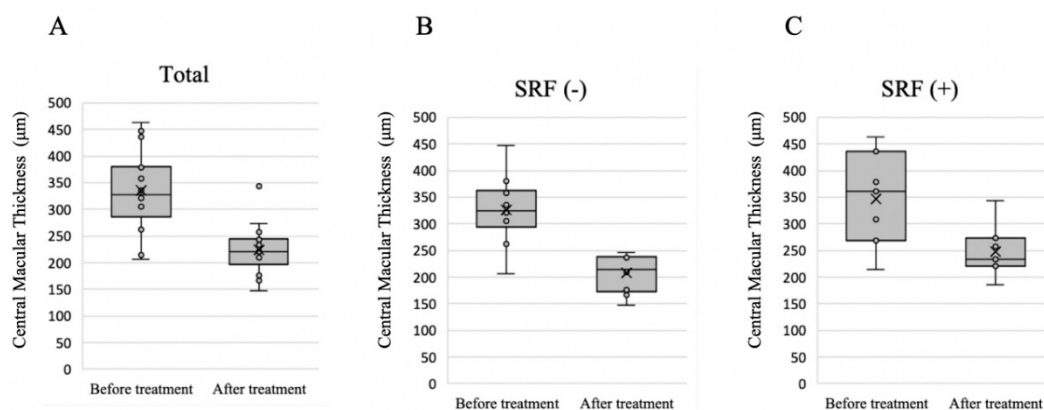


Figure 4. Changes in central macular thickness before treatment and 3 months after treatment. (A) Changes in central macular thickness in all 17 eyes. (B) Changes in central macular thickness in 10 eyes with no SRF 3 months after treatment. (C) Changes in central macular thickness in seven eyes with SRF 3 months after treatment. Significant differences in central macular thickness were observed before and after treatment in all groups. * $P < 0.001$, Wilcoxon signed-rank test. SRF: subretinal fluid.

3.3. Choroidal thickness before and after treatment

A significant decrease in choroidal thickness was observed after treatment in all nine areas ($P < 0.001$; **Table 3**). Additionally, we investigated whether the choroid was more likely to become thinner in the posterior (9-mm subfield) or peripheral (9–18-mm subfield) area. Results showed that choroidal thickness significantly decreased in the 9-mm subfield compared to that in the 9–18-mm subfield ($P = 0.002$; **Table 4**).

Table 3. Choroidal thickness before and after half-fluence PDT.

Areas	Before treatment	After treatment	P-value
3-mm subfield	359.1 ± 62.0	359.1 ± 62.0	<0.001
3–9-mm subfield	287.9 ± 48.1	253.5 ± 50.2	<0.001
Supratemporal 3–9 mm	348.8 ± 60.0	305.5 ± 58.5	<0.001
Infratemporal 3–9 mm	320.5 ± 66.9	278.1 ± 63.7	<0.001
Supranasal 3–9 mm	314.8 ± 72.6	287.1 ± 70.5	<0.001
Infranasal 3–9 mm	275.8 ± 59.3	244.4 ± 64.6	<0.001
9–18-mm subfield	236.1 ± 40.5	215.8 ± 38.9	<0.001
Supratemporal 9–18 mm	281.1 ± 54.9	255.9 ± 51.8	<0.001
Infratemporal 9–18 mm	233.1 ± 51.7	210.6 ± 47.7	<0.001
Supranasal 9–18 mm	252.1 ± 62.4	232.9 ± 59.7	<0.001
Infranasal 9–18 mm	178.1 ± 38.4	163.8 ± 36.3	<0.001

The data are shown as means with standard deviations. P-values were calculated using the Wilcoxon signed-rank test to compare choroidal thickness before and after treatment. PDT: photodynamic therapy.

Table 4. Ratio of change in choroidal thickness before and after treatment in the posterior and peripheral areas.

Areas	Before treatment	After treatment	Ratio	P-value
9-mm subfield	282.3 ± 53.1	258.5 ± 48.1	0.88 ± 0.07	0.002
9–18-mm subfield	222.6 ± 47.1	198.6 ± 49.0	0.91 ± 0.06	

The data are shown as means with standard deviations. P-values were calculated using the Wilcoxon signed-rank test.

As described above, we determined whether a dominant side exists for the deep choroidal vein and the vortex veins. If either the upper or lower direction was dominant, it was defined as an asymmetrical pattern; otherwise, it was defined as a symmetrical pattern. The choroidal thickness decreased in both the supratemporal and infratemporal 9x9-mm subfields in all three groups, and there was no significant difference in the ratio between them (Table 5).

Table 5. Difference in the ratio of change in choroidal thickness due to treatment between the dominant and non-dominant sides.

Asymmetrical pattern (n=11; upper dominant, n=8, lower dominant, n=3)				
Areas	Before treatment	After treatment	Ratio	P-value
Dominant side	273.5 ± 49.4	257.5 ± 53.0	0.94 ± 0.05	0.68
Non-dominant side	253.2 ± 36.6	237.8 ± 47.7	0.94 ± 0.05	
Symmetrical pattern (n=6)				
Areas	Before treatment	After treatment	Ratio	P-value
Upper area	270.5 ± 65.3	241.7 ± 64.4	0.89 ± 0.08	0.11
Lower area	186.5 ± 27.6	153.3 ± 36.0	0.83 ± 0.18	

The choroidal thickness in the supratemporal and infratemporal 9x9-mm subfields was analyzed. The data are shown as means with standard deviations. P-values were calculated using the Wilcoxon signed-rank test.

4. Discussion

This study demonstrated that half-fluence PDT with adjuvant aflibercept reduced choroidal thickness in both the central and peripheral areas using UWF-OCT analyses. Furthermore, the ratio of change in choroidal thickness was greater in the central area than in the peripheral area. We previously reported that the choroid was thicker in both the central and peripheral area in PNV compared to that in other nAMD subtypes and that the increased choroidal thickness was pronounced particularly in the central area [5]. Although the underlying mechanism for the reduction in choroidal thickness following PDT is not fully understood, our results suggest that the thickened choroid in PNV can be improved by PDT.

PDT addresses the underlying pachychoroid-based pathology rather than providing simple photocoagulation at the leakage points, as it has been shown to improve choroidal thickening and CVH in CSC [12]. The dynamic changes in choroidal blood circulation following PDT in PNV may shed light on its pathology. Accordingly, we analyzed the changes in choroidal thickness post-PDT using UWF-OCT.

In this study, the areas irradiated with PDT were located near the macula. It has been hypothesized that congestion in the vortex vein plays a role in the pathogenesis of CSC and PNV [21-23]. Consistently, various studies have reported a vertical asymmetry in the running pattern of deep choroidal veins in PSD [17, 23, 24]. To investigate the relationship between the dominant side of choroidal outflow from the macula and choroidal thickness, we identified the dominant side based on the location of the watershed zone. However, no correlation was observed between the reduction in choroidal thickness after PDT and the dominant side of the vortex vein. The decrease in choroidal thickness on the dominant side was not significantly different from that on the non-dominant side. This finding contrasts with those of previous studies on patients with CSC treated with PDT [20]. Further research, including a larger cohort of patients with PNV treated with PDT, is warranted. Additionally, evaluating the volumetric changes in the choroidal stroma versus the lumen post-PDT is crucial.

PDT may cause the occlusion of choriocapillaris [25], potentially causing choroidal thinning due to reduced blood flow from the choriocapillaris on the irradiated area. Although PDT was performed around the macular areas where the choroidal blood flowed to the dominant side, the choroidal thickness on the non-dominant side also decreased. Matsumoto et al. reported thinning of the choroid on the dominant side rather than on the non-dominant side after PDT in CSC [20]; however, our results in PNV cases were not consistent with those in CSC. A decrease in choriocapillaris blood flow occurred within the PDT-irradiated area [26]. Given that PDT is performed around the macular area, the choriocapillaris blood in the irradiated area should outflow to the vortex vein on the dominant side. Therefore, one might theoretically believe that deep choroidal blood flow decreases mainly on the dominant side [20]. However, choroidal vessels are intertwined and connected throughout the eyeball; therefore, it is not surprising that a reduction in luminal volume of the choroidal veins may occur throughout the choroid. An alternative hypothesis is that PDT could improve CVH through pathways other than the occlusion of the choriocapillaris, such as modifying growth factors (e.g. VEGF) or cytokine/chemokine signaling within the choroid [27, 28] and reducing its stromal and luminal volume.

Additionally, we investigated the factors associated with treatment outcomes after PDT and found no statistically significant factors. However, patients with remaining SRF tended to be older than those without SRF ($P = 0.11$). Therefore, older patients with PNV might exhibit greater resistance to PDT in ameliorating SRF. In this study, seven eyes (41.2 %) had SRF 3 months after PDT. The proportion of eyes with persistent SRF was higher than that previously reported in patients with CSC [29, 30]. Given that some cases of PNV can occur secondary to CSC [3, 31], younger patients with PNV may share similarities with patients with CSC in terms of fluid resolution by PDT. In contrast, PNV with a longer clinical course may be associated with RPE dysfunction, which is an important pathology of AMD. Future studies with a larger number of patients treated with PDT are required to clarify this further.

In this study, a single dose of aflibercept was administered prior to half-fluence PDT, which requires consideration of the residual effects of aflibercept in decreasing choroidal thickness. A single dose of aflibercept can reduce choroidal thickness, with a peak effect observed at 15 days post-injection [32]. However, there is no clear evidence regarding the extent to which the decreased choroidal thickness returns to the pre-treatment level 3 months after a single dose in AMD. Previous studies involving 144 patients treated with aflibercept showed that choroidal thickness continuously decreased with three loading doses, reducing to an average of 87% of the pretreatment level. The most significant decrease in choroidal thickness occurred 1 month after the first dose, and approximately 40% of the reduction caused by the first injection recovered 2 months after the third dose [33]. Furthermore, during bimonthly injections following the loading phase, fluctuations in choroidal thickness were observed between treatments [33]. These fluctuations indicated that the choroidal thickness nearly returned to its baseline level within 2 months. Therefore, theoretically, the reduction in choroidal thickness is presumed to recover 3 months after a single dose.

This study has some limitations. First, this was a single-center retrospective study with a relatively small number of patients receiving half-fluence PDT. A larger sample size may elucidate a clearer relationship between the presence of SRF at 3 months post-treatment and patient age. Findings regarding the patterns of deep choroidal veins and the reduction in choroidal thickness might change with a larger study population. In addition, the follow-up period after PDT was shorter. Although UWF-OCT was performed to analyze choroidal thickness, there were limitations in assessing areas, including the vortex vein ampulla, owing to the limited angle of view. A study analyzing the vortex vein area in patients with PNV would contribute to a better understanding of its pathology in future research.

In conclusion, treatment with half-fluence PDT decreased the entire choroidal thickness in patients with PNV, and no relationship was observed between reduction in choroidal thickness and the dominant side of the vortex vein. Our analysis of choroidal thickness using UWF-OCT, focusing on the treatment of PNV, may contribute to unraveling the mechanisms and pathogenesis of PDT in PSD.

Author Contributions: Y. F. and S. N. designed the study and drafted the manuscript. S. H. and K. F. analyzed and interpreted the data. Y. M. and K. Y. collected data. K. K. and S. S. edited the manuscript. K. I., T. H. and KH. S. critically reviewed the final version of the manuscript. All coauthors read and approved the final manuscript.

Funding: Funding: Japan Society for the Promotion of Science, Grant-in-Aid for Scientific Research; JP21K09702.

Institutional Review Board Statement: This retrospective study was approved by the Institutional Review Board of Kyushu University, Fukuoka, Japan, and adhered to the tenets of the Declaration of Helsinki.

Informed Consent Statement: Informed consent was obtained from all subjects involved in the study. Written informed consent has been obtained from the patients to publish this paper.

Data Availability Statement: All data generated or analyzed during this study are included in this article. Further inquiries can be directed to the corresponding author.

Acknowledgments: None

Conflicts of Interest: The authors declare no conflict of interest.

References

1. Pang, C.E. and K.B. Freund, Pachychoroid neovascularopathy. *Retina*, 2015. 35(1): p. 1-9.
2. Cheung, C.M.G., et al., Pachychoroid disease. *Eye (Lond)*, 2019. 33(1): p. 14-33.
3. Yanagi, Y., Pachychoroid disease: a new perspective on exudative maculopathy. *Jpn J Ophthalmol*, 2020. 64(4): p. 323-337.
4. Notomi, S., et al., Drusen and pigment abnormality predict the development of neovascular age-related macular degeneration in Japanese patients. *PLoS One*, 2021. 16(7): p. e0255213.
5. Fukuda, Y., et al., Differences in Central and Peripheral Choroidal Thickness among the Subtypes of Age-Related Macular Degeneration in an Asian Population. *J Clin Med*, 2023. 12(16).
6. Ishikura, M., et al., Widefield Choroidal Thickness of Eyes with Central Serous Chorioretinopathy Examined by Swept-Source OCT. *Ophthalmol Retina*, 2022. 6(10): p. 949-956.
7. Funatsu, R., et al., Choroidal morphologic features in central serous chorioretinopathy using ultra-widefield optical coherence tomography. *Graefes Arch Clin Exp Ophthalmol*, 2023. 261(4): p. 971-979.
8. Fung, A.T., L.A. Yannuzzi, and K.B. Freund, Type 1 (sub-retinal pigment epithelial) neovascularization in central serous chorioretinopathy masquerading as neovascular age-related macular degeneration. *Retina*, 2012. 32(9): p. 1829-37.
9. Matsumoto, H., et al., Efficacy of treat-and-extend regimen with aflibercept for pachychoroid neovascularopathy and Type 1 neovascular age-related macular degeneration. *Jpn J Ophthalmol*, 2018. 62(2): p. 144-150.
10. Schworm, B., et al., Vanishing pachy-choroid in pachychoroid neovascularopathy under long-term anti-vascular endothelial growth factor therapy. *BMC Ophthalmol*, 2021. 21(1): p. 269.
11. Sartini, F., et al., Pachychoroid neovascularopathy: a type-1 choroidal neovascularization belonging to the pachychoroid spectrum-pathogenesis, imaging and available treatment options. *Int Ophthalmol*, 2020. 40(12): p. 3577-3589.
12. Maruko, I., et al., Subfoveal choroidal thickness after treatment of central serous chorioretinopathy. *Ophthalmology*, 2010. 117(9): p. 1792-9.
13. Yamada-Okahara, N., et al., Practical treatment options for persistent central serous chorioretinopathy and early visual and anatomical outcomes. *Jpn J Ophthalmol*, 2023. 67(3): p. 295-300.
14. Kitajima, Y., et al., One-year outcome of combination therapy with intravitreal anti-vascular endothelial growth factor and photodynamic therapy in patients with pachychoroid neovascularopathy. *Graefes Arch Clin Exp Ophthalmol*, 2020. 258(6): p. 1279-1285.
15. Roy, R., et al., Treatment outcomes of pachychoroid neovascularopathy with photodynamic therapy and anti-vascular endothelial growth factor. *Indian J Ophthalmol*, 2019. 67(10): p. 1678-1683.
16. Spaide, R.F., H. Koizumi, and M.C. Pozzoni, Enhanced depth imaging spectral-domain optical coherence tomography. *Am J Ophthalmol*, 2008. 146(4): p. 496-500.
17. Hiroe, T. and S. Kishi, Dilatation of Asymmetric Vortex Vein in Central Serous Chorioretinopathy. *Ophthalmol Retina*, 2018. 2(2): p. 152-161.
18. Funatsu, R., et al., Effect of photodynamic therapy on choroid of the medial area from optic disc in patients with central serous chorioretinopathy. *PLoS One*, 2023. 18(2): p. e0282057.
19. Nishigori, N., et al., Extensive reduction in choroidal thickness after photodynamic therapy in eyes with central serous chorioretinopathy. *Sci Rep*, 2023. 13(1): p. 10890.
20. Matsumoto, H., et al., Attenuation of irradiated choroid and its regional vortex veins in central serous chorioretinopathy after photodynamic therapy. *Sci Rep*, 2023. 13(1): p. 19903.

21. Matsumoto, H., et al., Choroidal congestion mouse model: Could it serve as a pachychoroid model? *PLoS One*, 2021. 16(1): p. e0246115.
22. Matsumoto, H., et al., Vortex vein congestion in the monkey eye: A possible animal model of pachychoroid. *PLoS One*, 2022. 17(9): p. e0274137.
23. Hirooka, K., et al., Imbalanced choroidal circulation in eyes with asymmetric dilated vortex vein. *Jpn J Ophthalmol*, 2022. 66(1): p. 14-18.
24. Kishi, S. and H. Matsumoto, A new insight into pachychoroid diseases: Remodeling of choroidal vasculature. *Graefes Arch Clin Exp Ophthalmol*, 2022. 260(11): p. 3405-3417.
25. Schlötzer-Schrehardt, U., et al., Dose-related structural effects of photodynamic therapy on choroidal and retinal structures of human eyes. *Graefes Arch Clin Exp Ophthalmol*, 2002. 240(9): p. 748-57.
26. Demircan, A., C. Yesilkaya, and Z. Alkin, Early choriocapillaris changes after half-fluence photodynamic therapy in chronic central serous chorioretinopathy evaluated by optical coherence tomography angiography: Preliminary results. *Photodiagnosis Photodyn Ther*, 2018. 21: p. 375-378.
27. Hunt, D.W. and A.H. Chan, Influence of photodynamic therapy on immunological aspects of disease - an update. *Expert Opin Investig Drugs*, 2000. 9(4): p. 807-17.
28. Schmidt-Erfurth, U., et al., Influence of photodynamic therapy on expression of vascular endothelial growth factor (VEGF), VEGF receptor 3, and pigment epithelium-derived factor. *Invest Ophthalmol Vis Sci*, 2003. 44(10): p. 4473-80.
29. Shin, J.Y., et al., Comparison of efficacy and safety between half-fluence and full-fluence photodynamic therapy for chronic central serous chorioretinopathy. *Retina*, 2011. 31(1): p. 119-26.
30. Nicoló, M., et al., Half-fluence versus half-dose photodynamic therapy in chronic central serous chorioretinopathy. *Am J Ophthalmol*, 2014. 157(5): p. 1033-7.
31. Shiragami, C., et al., Clinical Features of Central Serous Chorioretinopathy With Type 1 Choroidal Neovascularization. *Am J Ophthalmol*, 2018. 193: p. 80-86.
32. Minnella, A.M., et al., Choroidal Thickness Changes After Intravitreal Aflibercept Injections in Treatment-Naïve Neovascular AMD. *Adv Ther*, 2022. 39(7): p. 3248-3261.
33. Koizumi, H., et al., Subfoveal Choroidal Thickness during Aflibercept Therapy for Neovascular Age-Related Macular Degeneration: Twelve-Month Results. *Ophthalmology*, 2016. 123(3): p. 617-24.

Disclaimer/Publisher's Note: The statements, opinions and data contained in all publications are solely those of the individual author(s) and contributor(s) and not of MDPI and/or the editor(s). MDPI and/or the editor(s) disclaim responsibility for any injury to people or property resulting from any ideas, methods, instructions or products referred to in the content.